Comparison of Aircraft Observations with Mixed-Phase Cloud Simulations

PAUL A. VAILLANCOURT,* ANDRÉ TREMBLAY, STEWART G. COBER, AND GEORGE A. ISAAC

Cloud Physics Research Division, Meteorological Service of Canada, Dorval, Quebec, Canada

(Manuscript received 23 January 2002, in final form 19 July 2002)

ABSTRACT

In order to provide guidance for the further improvement of a mixed-phase cloud scheme being developed for use in an NWP model, comparisons of dynamical, thermodynamical, and microphysical variables between in situ aircraft data and model data were made. A total of 21 flights (~88 h of data) from the First and Third Canadian Freezing Drizzle Experiments were selected and simulated. The basis of the evaluation of the model performance is a point-by-point comparison of each pertinent variable along the real and ''virtual'' aircraft trajectories. The virtual aircraft trajectory is constructed by choosing, for every observed data point, the closest available model data point in terms of time, pressure level, and latitude–longitude position. Observed and model data were used to calculate simple descriptive statistics to evaluate the ability of the forecast system to predict the presence of clouds, their phase, and water content.

Even though a point-by-point comparison of the aircraft and model data is a very severe test given the errors in the initial conditions and the disparity in temporal and spatial resolution, the results were encouraging for about half the flights simulated. It was found that, in general, the model predicts ice clouds better than water clouds. The model generally overpredicts (underpredicts) both the presence and the quantities of ice water content (supercooled liquid water content). Furthermore, where mixed-phase clouds are present in the model, the ice phase represents a large fraction of the total water content, contrary to the observations. These conclusions suggest that the parameterization of the ice particle size distribution is an important aspect of the mixed-phase cloud scheme that should be optimized.

1. Introduction

The presence of supercooled liquid water (SLW) in various types of cold clouds is very common. For example, Brown et al. (1997) counted over 14 000 pilot reports (PIREPs) reporting icing (freezing of supercooled drops on contact with a solid surface such as an aircraft) of various intensities over the continental United States during a 2-month period in the winter of 1994. There is also an abundance of detailed observations of SLW made in a cloud physics research context (e.g., Sand et al. 1984; Politovich 1989; Ashenden and Marwitz 1998; Cober et al. 2001a). Isaac et al. (1998, 2001) present an overview of the Canadian Freezing Drizzle Experiments (CFDE) I, II, and III and the Alliance Icing Research Study (AIRS) during which many aircraft measurements of SLW in both maritime and continental winter storm conditions were made with a special focus on environments containing drizzle-sized supercooled droplets. Hobbs and Rangno (1985) concluded from the examination of a broad database of research aircraft data (>160 clouds from maritime and continental locations) that the occurrence of a layer of SLW at cloud tops in both stratiform and cumuliform cold clouds was common. Such layers were found at temperatures as cold as −31°C (Rauber and Grant 1986). SLW has also been measured in cirrus (Sassen 1985) and orographic lenticular clouds (Heymsfield and Miloshevich 1993) at temperatures of ~−36°C. Furthermore, satellite data suggest that SLW also frequently occurs in deep layers of vigorous convective (preferentially continental) storms (Rosenfeld and Lensky 1998). The abundance of these observations suggests that liquid water droplets may be present in most cold clouds (given that the temperature is warmer than the threshold for homogeneous nucleation, ~>−40°C) at some point during their evolution.

There are three conditions for the formation of supercooled cloud water. The temperature must be <0°C, the relative humidity with respect to water must reach saturation, and if the ice phase is present, the condensate supply rate must exceed the ice crystal mass diffusional growth rate. Once formed, the fate of the supercooled cloud droplets can take several paths. In certain conditions, the SLW cloud droplets can grow by collision–coalescence to drizzle-or rain-sized drops and precipi-

* Current affiliation: Recherche en Prevision Numerique, Meteorological Service of Canada, Dorval, Quebec, Canada.

Corresponding author address: Dr. P. Vaillancourt, Recherche en Prévision Numérique, Meteorological Service of Canada, 2121 Trans-Canada Hwy., Dorval, QC H9P 1J3, Canada.
E-mail: paul.vaillancourt@ec.gc.ca

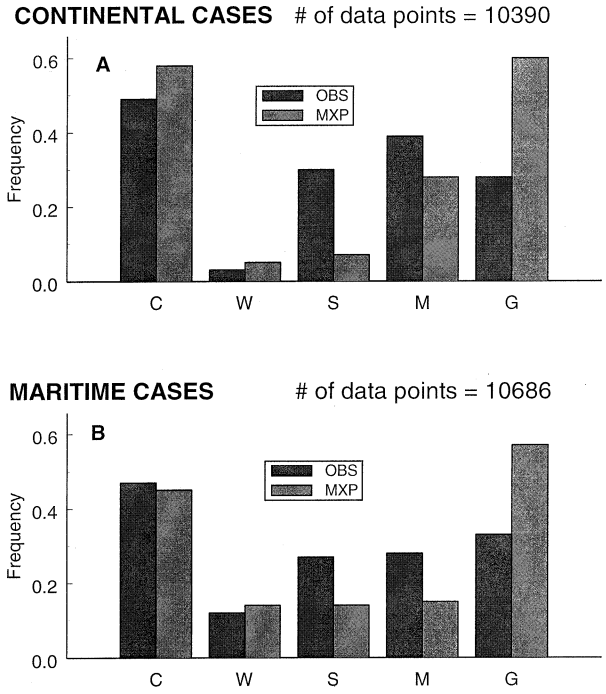

FIG. 1. The frequency of each cloudy type observed as well as modeled for the 10 continental cases (A) and the 11 maritime cases (B). The letters C, W, S, M, and G stand for clear (TWC < 0.02 g kg^{-1}), warm (temperature $> 0°$), supercooled (no ice is present), mixed, and glaciated (no liquid is present), respectively. The frequency for clear data points is normalized with the total number of data points indicated in each panel (same for observed and modeled data points), whereas the frequencies of the various cloudy types are normalized by the total number of nonclear data points (different for observed and modeled data points).

tate. For example, both Politovich (1989) and Cober et al. (1996) observed drizzle in shallow stratiform cloud systems with cloud-top temperatures $> -15°$C. Supercooled clouds can become glaciated if seeded with ice crystals sedimenting from an ice cloud at higher altitudes. Moreover, when SLW moves to a region where ice nucleation (homogeneous or heterogeneous) is active, the droplet population may evaporate and or glaciate. More research is necessary to understand how fast and under what conditions these various freezing mechanisms can glaciate a cloud region composed of SLW.

The formation and lifetime of SLW in clouds are important to study for several reasons. For example, it has been shown in Sassen et al. (1985) that SLW, sometimes found at the base of cirrus clouds, has a significant impact on the radiative transfer in these clouds. The presence of SLW clouds can cause in-flight icing on aircraft surfaces, and the associated loss of aircraft performance may result in accidents. For example, it is believed that the primary factor in the crash of an ATR-72 commuter aircraft near Roselawn, Indiana, in 1994 was the accumulation of ice, associated with supercooled large droplets, behind the aircraft's deicing boots (Marwitz et al. 1997). Several observations (Sand et al. 1984; Politovich 1989; Cober et al. 1996; Cober et al. 2001b) have shown that supercooled drizzle-sized drops are sometimes present in sufficient quantity in clouds to represent hazardous icing conditions.

Another impact of SLW in clouds is through its role in the generation of freezing precipitation (FP). From a climatological point of view, FP is a rare event [see Strapp et al. (1996) and Stuart and Isaac (1999) for a climatology of FP]. Over North America, it occurs most frequently in the eastern portion of Newfoundland (an annual average of 150 h of FP) and in the Great Lakes region (see also Cortinas 2000). Annual averages ranging between 10 and 50 h are typical for the rest of the continent. However, its dramatic impacts on human activity make it very important to forecast. An extreme example is the ice storm of January 1998 that hit densely populated regions of Ontario and Québec and caused 25 deaths and in excess of $1 billion in damages. During this event, the accumulation of freezing rain and ice pellets exceeded 100 mm in many areas of southwestern Quebec and eastern Ontario (Reagan 1998).

The supercooled drizzle or raindrops responsible for FP may originate either from the melting of solid hydrometeors in a warm air layer (classical mechanism) or may involve only the liquid phase (nonclassical mechanism). Several studies have examined radiosonde data from the North American World Meteorological Organization (WMO) network to determine the relative importance of these two mechanisms, based on the presence or the absence of a warm layer aloft. It is generally assumed that when a warm layer is present (absent) below the cloud that FP forms through the classical (nonclassical) mechanism. Huffman and Norman (1988) examined sounding data at 48 stations over a 10-yr period and found that about 30% of FP cases occur in the absence of a warm layer. Strapp et al. (1996) examined 22 yr of sounding data at three Canadian stations and found that the nonclassical mechanism was responsible for 38%–72% of FP events, depending on the location of the station. Rauber et al. (2000) extracted from a 25-yr database covering the United States east of the Rockies a total of 990 soundings from stations where FP was being reported. They found that 47% of FP events could be attributed to the nonclassical mechanism. Assuming that ice processes may be inactive when the cloud-top temperature is warmer than $-10°$C, they argued that this percentage may be as high as 75%. This implies that NWP parameterizations that diagnose precipitation type based only on the presence of a warm layer (e.g., Bourgouin 2000) will underforecast the occurrence of FP (in particular freezing drizzle).

In summary, a better understanding of the formation and lifetime of SLW is necessary both for better aircraft icing and FP forecasts.

2. Objectives

The present research is part of the ongoing effort of the Meteorological Service of Canada to provide useful

TABLE 1. The number of observed (OBS) and modeled (MXP) data points of each cloudy type for the 21 cases. The letters C, W, S, M, and G stand for clear (TWC < 0.02 g kg^{-1}), warm (temperature $> 0°$), supercooled (no ice is present), mixed, and glaciated (no liquid is present), respectively. The last column (D) shows the number of data points where drizzle was observed.

	Date	MXP C	OBS C	MXP W	OBS W	MXP S	OBS S	MXP M	OBS M	MXP I	OBS I	Sum	OBS D
c1	15 Dec 1997	605	485	0	1	78	143	30	160	87	11	800	198
c2	8 Jan 1998	150	131	216	121	136	160	190	193	297	384	989	326
c3	13 Jan 1998	52	108	0	24	0	58	278	477	485	148	815	8
c4	15 Jan 1998	239	459	0	0	4	191	429	324	448	146	1120	180
c5	17 Jan 1998	1057	679	0	0	16	130	0	110	0	154	1073	72
c6	19 Jan 1998	684	576	0	0	1	42	19	143	204	147	908	0
c7	22 Jan 1998	967	787	0	0	52	378	184	70	34	2	1237	156
c8	24 Jan 1998	1100	561	0	0	0	272	0	267	0	0	1100	118
c9	11 Feb 1998	157	597	2	0	0	22	61	145	886	342	1106	0
c10	17 Feb 1998	1050	738	0	0	6	186	18	158	168	160	1242	122
	Sum	6061	5121	218	146	293	1582	1209	2047	2609	1494	10 390	1180
m1	3 Mar 1995	204	196	68	41	140	52	70	443	521	271	1003	136
m2	6 Mar 1995	139	836	124	77	14	86	74	24	685	13	1036	64
m3	7 Mar 1995	333	647	68	71	3	155	319	111	317	56	1040	172
m4	8 Mar 1995	735	293	6	10	16	77	8	195	33	223	798	14
m5	9 Mar 1995	487	569	117	108	398	339	20	22	16	0	1038	408
m6	10 Mar 1995	121	338	130	84	234	129	86	191	382	211	953	291
m7	14 Mar 1995	589	787	211	232	14	83	44	11	268	13	1126	234
m8	15 Mar 1995	474	348	21	0	4	177	97	98	41	14	637	112
m9	17 Mar 1995	718	465	3	0	16	312	23	55	182	110	942	70
m10	18 Mar 1995	713	351	36	74	2	50	18	154	380	520	1149	105
m11	22 Mar 1995	285	215	11	6	0	67	144	266	524	410	964	132
	Sum	4798	5045	795	703	841	1527	903	1570	3349	1841	10 686	1738
	All cases	10 859	10 166	1013	849	1134	3109	2112	3617	5958	3335	21 076	2918

and reliable forecasts of aircraft icing and freezing precipitation. Since the current operational cloud scheme used in the Canadian forecast system does not allow predictions of SLW, the diagnostic technique proposed by Tremblay et al. (1995) is employed to produce icing forecasts. This technique, however, provides only information on the presence or absence of SLW in clouds and it is impossible to determine the intensity of a SLW event. To improve this, Tremblay et al. (1996) developed a mixed-phase scheme (MXP) that is computationally fast and easy to implement in a mesoscale or large-scale atmospheric model. The scheme solves a prognostic equation for the total water content (TWC) and a diagnostic is used to obtain its partition between the solid and liquid phase. A noteworthy point is that an explicit cloud scheme such as the MXP scheme allows a more physical coupling between the dynamics, cloud processes, radiation, and the hydrological cycle in the forecast model. The MXP scheme has been successfully verified against satellites, radiosondes, and surface observations (Tremblay and Glazer 2000) and compared to the current operational cloud scheme as well as to a more sophisticated cloud scheme (Tremblay et al. 2001; Guan et al. 2002). It was found in these papers that the MXP scheme performed better than the current operational cloud scheme. In particular, MXP has better clouds, precipitation, and moisture forecasts.

There exists a whole variety of microphysical schemes of various complexities ranging from simple diagnostic schemes to bulk schemes that prognose one or more moments of one or more types of hydrometeors, to the so-called explicit schemes that solve for the evolution and interaction among various hydrometeors using the spectral (bin) approach (see Khain et al. 2000 for a review). Choosing the necessary level of complexity of the microphysical scheme is not an obvious exercise. It must be a function of the resolution of the model as well as the type of phenomena under consideration. Furthermore, while more complex schemes represent the physics of clouds in a more realistic fashion, they remain highly parameterized schemes sensitive to many tunable parameters. Comparisons of the MXP scheme with a more complex scheme reported in Tremblay and Glazer (2001) and in Guan et al. (2002) as well as comparisons with other more complex schemes (not reported) have convinced us that in the context of a NWP model with mesoscale resolution, the complexity of the MXP scheme is sufficient.

In order to validate other aspects of this scheme and to provide guidance for its further improvement, point-by-point comparisons of dynamical, thermodynamical, and microphysical variables between in situ aircraft data and model data were made. More specifically, this research is aimed at answering the following questions:

1) How well do the model simulations forecast the position of clouds? Within clouds, how well does the MXP scheme forecast the phase of clouds?
2) Are ice water content (IWC) and liquid water content (LWC) in clouds properly forecast, in particular for supercooled water?

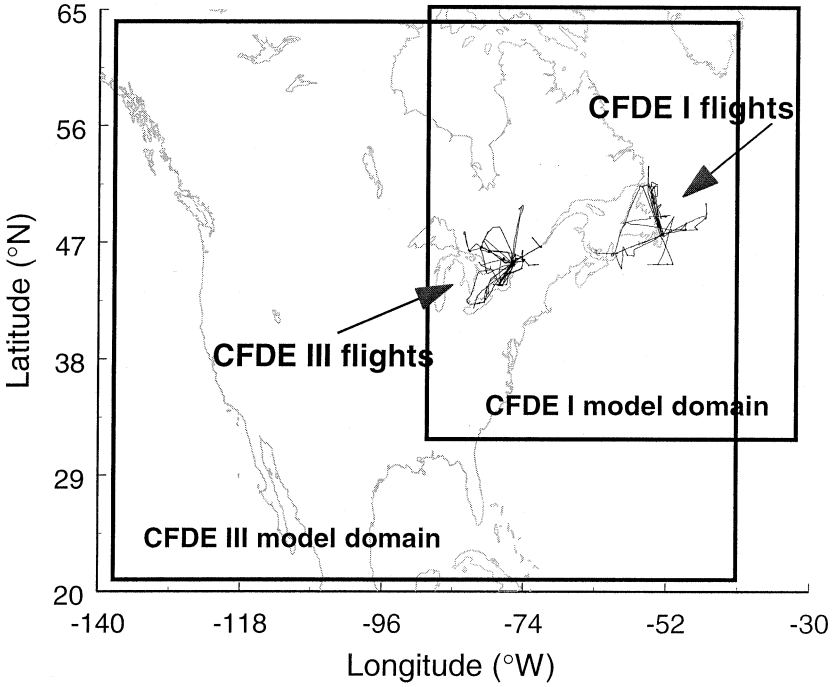

FIG. 2. The simulation domain for the maritime cases (CFDE I) and for the continental cases (CFDE III). Also shown are the flight paths of the selected flights centered in St. John's for the CFDE I flights and in Ottawa for the CFDE III flights.

3) In mixed-phase conditions, does the MXP scheme reproduce the observed climatology of the partition between ice and liquid water?
4) What are the weaknesses in MXP that should be addressed?

3. Dataset

Research aircraft data from two field experiments, CFDE I and III, are used for the comparison. CFDE I was conducted during March 1995 out of St. John's, Newfoundland. This campaign comprised 12 research flights for a total of 60 h of data. Eleven of these flights were selected for comparison with the model simulations (referred to as the maritime cases). CFDE III was conducted out of Ottawa from December 1997 to February 1998. This campaign comprised 26 research flights for a total of 105 h of data. Ten of these flights were selected for comparison with the model simulations (referred to as the continental cases). The flights selected were those that were the longest (between 3.5 and 5.5 h) and contained the most cloudy data points. Information on the research aircraft and its instrumentation can be found in Isaac et al. (2001) and Cober et al. (2001a,b). The aircraft data used are 15-s averages, representing a length scale of ~1.5 km. For the 21 flights selected, this represents a total of ~21 000 data points or ~88 h.

The histograms presented in Fig. 1 (see also Table 1) show the frequency of occurrence of each cloudy type observed as well as modeled (discussed in the next section) for all continental and maritime cases. Note that the frequency for clear data points was normalized to the total number of data points, whereas the frequencies of the nonclear data points were normalized to the total number of nonclear data points. For both the maritime and the continental cases, approximately half of the observed data points were assessed as being out of cloud (i.e., TWC < 0.02 g kg^{-1}). For the observed cloudy data points, approximately 28% (33%) contained only ice crystals (G), 30% (27%) contained only supercooled liquid water (S), 39% (28%) contained both SLW and ice crystals (M), and 3% (12%) contained warm liquid water (W) (temperature > 0°C) for the continental (maritime) cases, respectively. Furthermore, approximately 22% (31%) of the cloudy points contain droplets larger than 100 μm in diameter (see Table 1 for exact number of data points for every flight). This percentage increases to 31% (46%) if the glaciated data points are excluded.

The aircraft data, as well as other data such as ground-based radars or soundings when available, were carefully examined to determine the origin of the SLW for each data point where SLW is present. For a minimum of 75% of such data points, the SLW cannot be imputed to the supercooling of melted ice crystals. This again reinforces the necessity of a cloud scheme that explicitly solves for water content and its sedimentation versus a scheme that would diagnose freezing precipitation based on the presence of a warm layer. Further details on phase

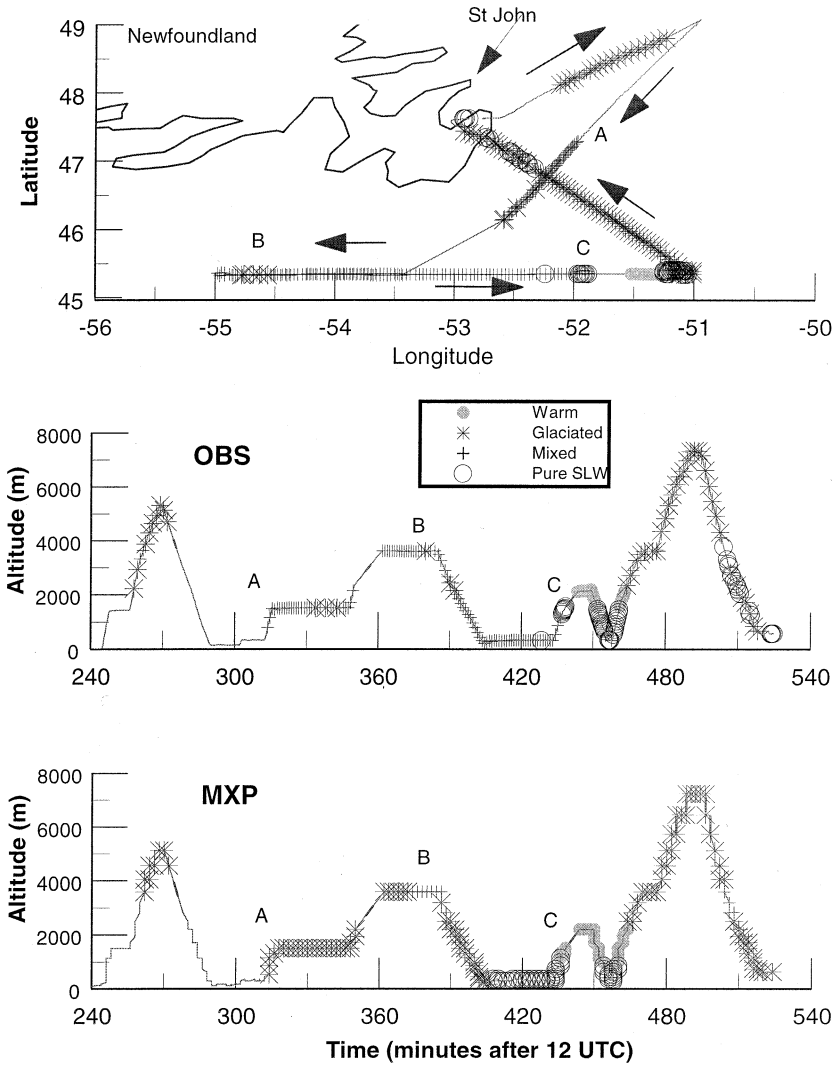

FIG. 3. (top) The aircraft trajectory as well as a comparison of the (middle) observed and (bottom) modeled cloud types along the trajectories shown on altitude vs time plots for the 3 Mar 1995 CFDE I flight (m1). The definition of the symbols identifying the cloud types shown in the three panels can be found in the middle panel.

assessment and differences between CFDE III and I can be found in Cober et al. (2001a).

4. Model and experimental procedure

The MXP scheme is used within the 3D, fully compressible, nonhydrostatic Mesoscale Compressible Community (MC2) dynamical model (Benoit et al. 1997). Some characteristics of this model include the semi-implicit semi-Lagrangian time scheme, variable vertical resolution, a terrain-following vertical coordinate, and a limited-area one-way nesting strategy. The model physics package (parameterizations of physical processes unresolved by the finite grid size) includes atmospheric surface layer exchanges, boundary layer turbulent transfer, solar and infrared radiation fluxes and their interaction with clouds, deep and shallow convective processes, gravity wave drag, and explicit prognosis of TWC (MXP scheme).

All simulations were 24-h-long runs initialized at 0000 UTC from the Canadian Meteorological Center (CMC) analysis. Most flights occurred after 1400 UTC, leaving a minimum period of 14 h for cloud spinup. The horizontal grid resolution was ~35 km (corresponding to the resolution of the analysis) and the time step was 2 min. Numerous experiments with the MXP scheme done in the context of the work presented in Tremblay et al. (2003) have demonstrated that a 2-min time step is more than adequate to resolve structures developing at the given horizontal resolution. In the vertical, 40 levels were used to obtain a vertical resolution varying from 50 m near the surface, to 150 m at

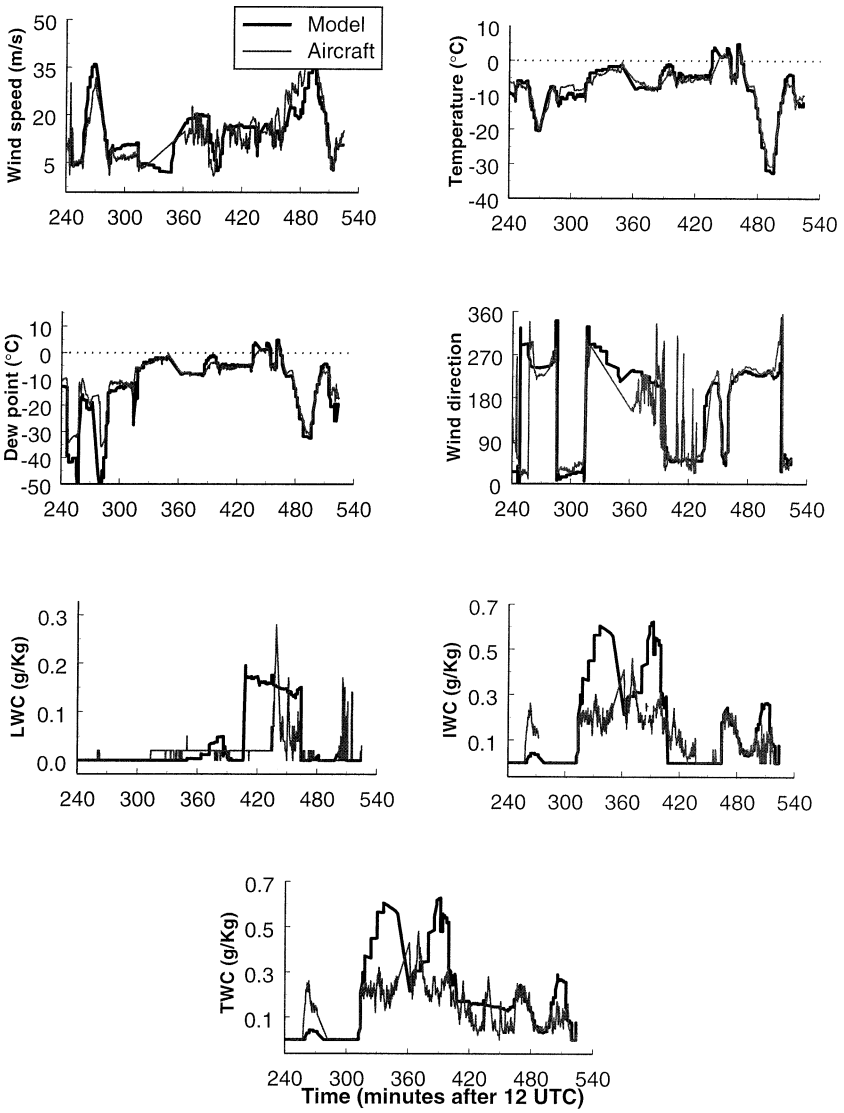

FIG. 4. Comparison of the observed (thin line) and modeled (thick line) time series of the wind speed, temperature, dewpoint temperature, wind direction, and total, ice, and liquid water content for the 3 Mar 1995 CFDE I flight (m1). The abscissa in all panels denotes time in minutes after 1200 UTC.

1 km, to 500 m at 5 km, and down to 2 km near the lid of the model situated at 25 km. Since sedimentation of either liquid or solid condensate is treated explicitly within the MXP scheme, a fractional time step is used to solve for sedimentation. This is necessary for the high-resolution levels near the surface.

The simulation domains for both sets of flights are shown in Fig. 2. The CFDE I simulations were performed on a 110 × 110 grid covering the northeast portion of the North American continent as well as part of the North Atlantic Ocean. The CFDE III simulations were performed on a 216 × 154 grid covering most of the North American continent.

The basis of the evaluation of the model performance is a point-by-point comparison of each pertinent variable along the real and ''virtual'' aircraft trajectories. The model is input with the aircraft trajectory in terms of the latitude–longitude points. For each of these points the model calculates the closest grid point. During its execution, the model outputs specified variables (e.g., wind, temperature, dewpoint temperature, total water content, and fractional ice water content) at all vertical levels and every time step for all such grid points. After model execution, the virtual aircraft trajectory is constructed by choosing, for every observed data point, the closest available model data point in terms of time, pressure level, and latitude–longitude position.

It is necessary to discuss the mismatch between the model's spatial and temporal resolution with the spatial and temporal resolution of the observations. With a 35-

TABLE 2. Descriptive statistics for each maritime (m) and continental case (c) for temperature, dewpoint temperature, and wind speed. The bias is defined as the model mean − the observed mean. Mean absolute error refers to the mean of the absolute value of the difference between the observed and modeled value. Sample refers to the total number of data points, while no. in models and no. in observations refer to the total number of data points where the given water content variable is nonzero.

	m1	m2	m3	m4	m5	m6	m7	m8	m9	m10	m11
					Temperature						
Correlation	0.97	0.98	0.97	0.95	0.97	0.97	0.99	0.97	0.97	0.97	0.96
Model mean	−7.9	−9.0	−8.5	−3.8	−4.7	−6.7	−5.1	−3.7	−6.3	−4.3	−6.2
Observed mean	−8.1	−9.8	−8.2	−6.9	−3.4	−6.6	−3.7	−5.3	−6.5	−4.8	−6.5
Bias	0.2	0.7	−0.2	3.1	−1.3	−0.1	−1.4	1.6	0.2	0.4	0.3
Mean absolute error	1.6	1.7	2.0	3.2	2.1	1.8	2.0	2.1	1.0	0.9	1.1
Sample	1051	1158	1130	800	1079	997	1158	859	1131	1179	989
					Dewpoint						
Correlation	0.95	0.89	0.87	0.85	0.84	0.91	0.91	0.61	0.82	0.86	0.74
Model mean	−12.2	−10.6	−12.5	−9.2	−9.0	−8.9	−9.4	−10.0	−9.7	−7.1	−9.2
Observed mean	−10.6	−14.4	−13.8	−7.2	−9.2	−8.1	−7.0	−13.1	−8.2	−5.1	−6.4
Bias	−1.6	3.8	1.3	−2.0	0.3	−0.8	−2.4	3.1	−1.4	−2.0	−2.7
Mean absolute error	2.9	4.8	5.1	3.9	4.0	3.1	4.1	7.8	3.3	2.7	3.7
Sample	1051	1158	1130	800	1079	997	1158	859	1131	1179	989
					Wind (m s^{-1})						
Correlation	0.31	0.62	0.76	0.68	0.92	0.77	0.79	0.40	−0.08	0.35	0.89
Model mean	14.2	22.2	17.7	23.6	23.9	24.6	15.6	6.9	5.5	5.9	18.3
Observed mean	17.8	19.5	19.4	33.9	26.8	28.4	16.6	10.9	5.0	12.0	18.1
Bias	−3.5	2.6	−1.7	−10.2	−2.8	−3.8	−1.0	−3.9	0.5	−6.1	0.2
Mean absolute error	7.4	5.1	6.8	12.2	4.3	7.7	3.5	4.7	3.0	6.1	3.4
Sample	1051	1145	1102	800	1073	937	1158	859	1131	1176	965

km grid box, there is a maximum distance of 25 km between the aircraft position and the closest model grid point when the aircraft is near the center of the grid box. While such a mismatch could be significant in summer or convective weather, it is less important for the large-scale stratiform winter clouds under study here. Higher-resolution simulations would likely increase the level of detail of the modeled systems, by producing better-defined fronts and transition zones between various types of precipitation. However since the objective here is not to look at the precise structure of individual systems but rather evaluate the ''climatology'' of the MXP scheme over as many weather systems as possible, horizontal resolution is less of an issue. Furthermore, a series of simulations (CFDE I flights) at a resolution of 7 km did not show any significant improvement in the model–aircraft comparison. Tremblay et al. (2003) obtained similar results and noted that increasing model resolution from 35 to 3 km with a nesting strategy did not change the quality of a winter storm forecast. This is probably to be expected given that the effective resolution of the initial conditions provided by the analysis is of the order of 200 km [directly related to the density of the observation network and the data assimilation technique—Laroche et al. (1999)]. Possibly more critical to this work is the vertical resolution. Because the aircraft is often descending or ascending and since the temperature gradient is much greater in the vertical than in the horizontal and since the temperature is critical in determining the phase of the hydrometeors, an adequate distribution of the model vertical levels should be selected. The average ascent or descent rate of the Convair-580 research aircraft is about 4 m s^{-1}. For 15-s data averages, this implies an approximate 60-m vertical resolution for the observations. This is comparable to the vertical resolution of the model at low levels (where most of the clouds were sampled by the research aircraft), implying that the present model setup is adequate.

Note that there are many other possible model–observation comparison strategies, with each strategy having its own advantages and disadvantages. For example, Guan et al. (2001) opted to interpolate the model output toward the frequency of the observations while Guan et al. (2002) opted to filter the observations toward the model's spatial resolution. In this paper, the choice was made to minimize the manipulation of the observations or of the model data. This choice allowed us to avoid filtering of observations toward the model's spatial or temporal resolution or interpolation of the model output toward the spatial or temporal scale of the observations.

Given that the performance of an NWP model is dependent on many aspects (e.g., initial conditions, resolution, physical parameterizations), this model–aircraft point-by-point comparison constitutes a very severe test for an NWP model and a cloud scheme. In particular, given the very coarse resolution of the initial conditions, the timing and position of the modeled meteorological systems should not be expected to be exact. Since the objective is to improve the MXP cloud scheme, the research was focused on identifying weaknesses that can be specifically imputed to it rather than to some other aspect of the complex NWP model. This is not an obvious exercise since the dynamics and the microphysics are strongly coupled.

TABLE 2. *(Extended)*

c1	c2	c3	c4	c5	c6	c7	c8	c9	c10
0.79	0.98	0.95	0.99	0.74	0.98	0.99	0.66	0.99	0.96
−3.9	−6.7	−5.1	−10.7	−7.9	−14.9	−11.7	−2.9	−13.0	−12.1
−4.9	−7.2	−6.0	−10.7	−8.5	−15.0	−11.7	−5.3	−12.0	−11.9
1.0	0.6	0.8	0.0	0.5	0.1	0.0	2.4	−1.1	−0.2
1.9	1.2	1.5	1.2	1.7	0.9	1.0	2.5	1.5	1.4
892	995	819	1142	1146	912	1259	1154	1135	1272
0.84	0.97	0.85	0.97	0.92	0.96	0.98	0.66	0.96	0.82
−8.0	−7.3	−5.4	−11.9	−20.7	−16.9	−17.7	−12.3	−14.2	−18.1
−11.0	−7.1	−6.0	−12.9	−15.7	−15.9	−15.8	−6.3	−13.4	−13.3
3.1	−0.2	0.5	1.0	−4.9	−1.0	−1.9	−6.0	−0.8	−4.8
3.5	1.5	1.7	2.1	5.3	1.9	2.9	6.3	2.0	5.3
892	995	819	1142	1146	912	1259	1154	1135	1272
0.88	0.78	0.42	0.94	−0.01	0.40	0.90	0.59	0.68	0.47
14.7	18.0	22.1	19.7	4.6	3.9	10.6	7.0	15.7	7.7
14.7	20.8	20.5	21.1	7.7	5.8	9.9	5.2	17.6	21.8
0.0	−2.8	1.6	−1.4	−3.1	−1.9	0.7	1.8	−1.9	−14.1
2.9	4.2	4.5	4.1	3.8	2.6	2.2	2.3	5.4	15.0
892	995	819	1142	1146	910	1259	1154	1132	889

Our strategy was to first draw general conclusions on the entire ''forecasting system'' based on the comparison of all cases, irrespective of the quality of the model simulation. Then we eliminated all cases where it was relatively obvious that the model simulation misplaced or misrepresented the weather systems. Such problems resulted in complete lack of clouds in the virtual aircraft trajectory or severe errors in their position. From the cases where all six compared variables were ''relatively good'' (in the quantitative and qualitative sense), we derived general conclusions pertinent for the microphysical scheme.

5. Results

Results for the comparison of the 21 real and virtual flights are presented in this section. The ability of the simulations in reproducing the observations was first evaluated qualitatively by comparing, for each flight, the time series of the following observed and model variables: cloud type, temperature, wind speed, wind direction, dewpoint temperature, TWC, IWC, and LWC. Such a comparison will be presented in detail for a single flight (CFDE I, 3 March 1995). A detailed analysis of one other flight (CFDE III, 15 January 1998) can be found in Tremblay et al. (2003). The success of the model–observation comparison was quantified by calculating simple statistics such as the correlation, bias, and average absolute errors. Based on these statistics, the 10 most successful simulations were selected for a more comprehensive analysis of the results. This analysis includes a comparison of the real and virtual ''climatologies'' of the cloud types as well as of the total, ice, and supercooled water content.

Figure 3 shows the aircraft trajectory as well as a comparison of the observed and modeled cloud types along the trajectories shown on altitude versus time plots for the CFDE I (3 March 1995) flight (case m1). The aircraft flew out of St. John's, Newfoundland, into the cloudy region ahead of an approaching warm front associated with a low pressure system south of Newfoundland. The aircraft first flew northeast where it sampled some glaciated clouds that were approximately 3000 m deep. It then turned and flew southwest until a point south of the Avalon Peninsula. On this leg the aircraft sampled (starting at point A) predominantly mixed-phase clouds. The aircraft then flew along an east–west path where it again mainly encountered mixed-phase clouds extending from an altitude of 4000 m to the surface. It also sampled some pockets of glaciated clouds near point B. The aircraft then gained altitude and encountered some pure SLW (point C) below a 1000-m-deep warm layer. At approximately 460 min, the aircraft turned to fly northwest where it sampled glaciated clouds and some pure SLW clouds on its approach to St. John's. The comparison of the aircraft observations and model output shows that, for this case, the model has done a satisfactory job in terms of the position and phase of clouds. However, several differences can be seen. From points A to B, the aircraft essentially observed mixed-phase conditions whereas the model produced glaciated clouds. On the other hand, around 425 min the aircraft saw mixed-phase conditions near the surface whereas the model produced pure SLW.

TABLE 3. Same as in Table 2 but for the TWC, the IWC, and the LWC.

	m1	m2	m3	m4	m5	m6	m7	m8	m9	m10	m11
					IWC (g kg^{-1})						
Correlation	0.71	0.09	0.31	0.39	−0.03	0.56	−0.08	0.25	0.65	0.41	0.62
Model mean	0.172	0.153	0.307	0.004	0.004	0.142	0.015	0.014	0.008	0.021	0.091
Observed mean	0.118	0.001	0.025	0.063	0.001	0.036	0.001	0.034	0.007	0.039	0.087
Bias	0.054	0.152	0.282	−0.059	0.003	0.105	0.014	−0.020	0.001	−0.018	0.004
Mean absolute error	0.102	0.152	0.282	0.059	0.005	0.124	0.017	0.041	0.007	0.032	0.057
Sample	1003	1036	1040	798	1038	989	1126	637	942	1149	964
No. in models	600	819	714	41	42	468	312	194	214	405	668
No. in observations	714	37	167	418	22	402	24	112	165	674	676
					TWC (g kg^{-1})						
Correlation	0.70	0.39	0.47	0.23	0.53	0.57	0.23	0.11	−0.06	0.43	0.33
Model mean	0.208	0.176	0.337	0.006	0.054	0.212	0.034	0.027	0.010	0.024	0.098
Observed mean	0.128	0.029	0.059	0.093	0.066	0.063	0.024	0.081	0.059	0.059	0.125
Bias	0.080	0.148	0.278	−0.087	−0.011	0.150	0.010	−0.054	−0.049	−0.035	−0.027
Mean absolute error	0.106	0.157	0.278	0.088	0.049	0.155	0.034	0.088	0.058	0.048	0.093
Sample	1003	1036	1040	798	1038	989	1126	637	942	1149	964
No. in models	808	1001	793	63	583	840	548	237	241	458	694
No. in observations	807	200	393	505	469	615	339	289	477	798	749
					LWC (g kg^{-1})						
Correlation	0.48	0.12	0.24	−0.09	0.52	0.35	0.15	0.00	0.02	0.35	−0.13
Model mean	0.036	0.024	0.031	0.002	0.051	0.071	0.019	0.013	0.002	0.003	0.007
Observed mean	0.011	0.028	0.034	0.030	0.065	0.026	0.023	0.047	0.052	0.020	0.038
Bias	0.025	−0.004	−0.004	−0.028	−0.014	0.044	−0.004	−0.034	−0.050	−0.016	−0.031
Mean absolute error	0.031	0.039	0.045	0.032	0.048	0.064	0.029	0.052	0.053	0.019	0.043
Sample	1003	1036	1040	798	1038	989	1126	637	942	1149	964
No. in models	285	266	459	30	566	458	280	193	56	75	170
No. in observations	243	187	303	228	469	376	326	223	367	278	286

Figure 4 shows a comparison of the observed and modeled time series of several variables for the same flight. It can be seen that, in this case, there is a good correspondence between the observed and modeled variables. In particular the simulated temperature, dewpoint temperature, and wind direction fit very closely to the observations. In the model, as in the observations, clouds are present throughout most of the trajectory and the water content signal is dominated by the ice water content. However the model generally overpredicts the IWC. Furthermore, the model does not predict the maximum in LWC observed at ~440 min. Instead, the modeled liquid water content signal saturates at a value of ≤ 0.2 g kg^{-1}. It will be shown later that this is a systematic property of the MXP scheme.

Figures 3 and 4 show a case where the model–observation scheme was a success in the sense that the dynamic variables, the presence of clouds, and their phase were well simulated. This success can partly be attributed to the fact that the aircraft sampled a region well within a vast cloudy area ahead of a warm front. In this situation, the model–observation comparison is somewhat ''protected'' from errors in the position of the modeled system. The model–observation comparison is much more sensitive to such errors when the aircraft sampled regions near the edges of storms.

Descriptive statistics are presented to summarize the comparisons between the model and the observations for the 21 cases. The first panel in Table 2 shows the correlation between the observed and modeled temperature as well as the model average, the observed average, the bias (model average–observed average), and the average of the absolute value of the difference between the observed and modeled data points for all selected maritime (denoted with m) and continental cases (denoted with c). Tables 2 and 3 also show the same statistics for the dewpoint temperature, the wind speed, the ice water content, the total water content, and the liquid water content. Note that the variables in Tables 2 and 3 are ordered as a function of decreasing correlation. In other words, the correlation for temperature is in general better than the correlation for dewpoint temperature, which is in general better than the correlation for wind speed. Table 4 contains the average, over all cases, for each statistic and for each variable listed above.

As can be seen in Tables 2 and 3, the correlations for temperature and dewpoint temperature are in general very good. No systematic biases in temperature or dewpoint temperature are apparent. Table 4 shows that the ''global'' bias of temperature is only 0.3°C whereas there is a negative bias (model is drier) of −1.0°C for the dewpoint temperature. Although the correlation for

TABLE 3. *(Extended)*

c1	c2	c3	c4	c5	c6	c7	c8	c9	c10
0.11	0.53	0.36	0.08	−0.17	0.19	0.07	−0.13	0.57	0.02
0.010	0.054	0.119	0.078	0.002	0.013	0.011	0.001	0.071	0.008
0.004	0.063	0.090	0.016	0.008	0.011	0.001	0.005	0.049	0.020
0.005	−0.009	0.028	0.062	−0.006	0.002	0.010	−0.004	0.022	−0.012
0.009	0.043	0.071	0.069	0.010	0.013	0.011	0.006	0.054	0.024
800	989	815	1120	1073	908	1237	1100	1106	1242
117	493	767	899	0	227	218	0	947	186
171	591	625	470	264	290	72	267	487	318
−0.02	0.21	0.47	0.60	−0.13	0.16	0.30	−0.24	0.62	−0.11
0.016	0.095	0.133	0.092	0.003	0.014	0.019	0.001	0.074	0.009
0.054	0.100	0.151	0.087	0.054	0.023	0.044	0.060	0.059	0.051
−0.038	−0.005	−0.018	0.005	−0.051	−0.009	−0.026	−0.059	0.015	−0.042
0.055	0.074	0.072	0.060	0.056	0.025	0.041	0.061	0.056	0.054
800	989	815	1120	1073	908	1237	1100	1106	1242
195	845	767	903	16	228	271	0	949	192
315	873	707	661	394	332	450	539	509	504
0.09	0.41	0.16	0.30	−0.09	0.01	0.30	−0.03	0.36	−0.06
0.007	0.041	0.015	0.014	0.001	0.001	0.007	0.000	0.003	0.001
0.050	0.037	0.061	0.072	0.046	0.013	0.043	0.056	0.010	0.031
−0.043	0.005	−0.047	−0.058	−0.046	−0.012	−0.036	−0.056	−0.006	−0.031
0.049	0.038	0.056	0.067	0.047	0.013	0.041	0.056	0.009	0.032
800	989	815	1120	1073	908	1237	1100	1106	1242
108	548	278	433	16	20	237	0	63	24
304	458	541	505	240	182	448	539	163	336

wind speed is also, in general, good, it is not as good as that for temperature and dewpoint temperature.

Examining Tables 2–4, it is apparent that it is more challenging to predict the water contents than the dynamic variables. It can be seen that the correlations for the water contents are smaller than those for the dynamic variables. Only 11 out of the 21 cases have a correlation greater than 0.3 for TWC. Among the water content variables, the correlations for IWC are the highest, implying that the model predicts ice clouds better than liquid clouds. Table 4 also shows that the model tends to overpredict the IWC (and the TWC) while underpredicting the LWC. Note that the means shown in this table are for the entire time series and not only in-cloud means. However, renormalizing the water contents to obtain the in-cloud values leads to the same conclusion. The statistics for SLW shown in Table 4 show that, over all cases, both the presence and quantity of SLW are strongly underestimated in the model.

We are aware that the quality of a model prediction cannot be reduced to two or three numbers. However, we have found that these simple statistics generally confirm our subjective evaluation of the forecasts based on a detailed visual inspection of the graphs of each flight. Furthermore, it should be noted that although linear correlations are perhaps not the most appropriate statistical tool to use in the context of variables that do not follow a normal distribution, such as the water contents, additional tests with other types of statistical tools (rank correlations, contingency table analysis) did not give very different results and confirmed the present conclusions.

TABLE 4. Same is in Table 2 but for the 21 cases combined. Also included are the descriptive statistics for the SLWC.

	Temp	Dewpoint	Wind (m s^{-1})	IWC (g kg^{-1})	TWC (g kg^{-1})	LWC (g kg^{-1})	SLWC (g kg^{-1})
Correlation	0.97	0.87	0.76	0.36	0.29	0.14	0.12
Model mean	−7.5	−11.6	14.2	0.062	0.078	0.016	0.011
Observed mean	−7.8	−10.6	16.4	0.031	0.068	0.037	0.033
Bias	0.3	−1.0	−2.2	0.031	0.01	−0.021	−0.022
Mean absolute error	1.6	3.7	5.1	0.056	0.081	0.041	0.036
Sample	22 221	22 221	21 699	21 076	21 076	21 076	21 076
No. in models				8331	10 632	4565	3439
No. in observations				6966	10 925	7002	6153

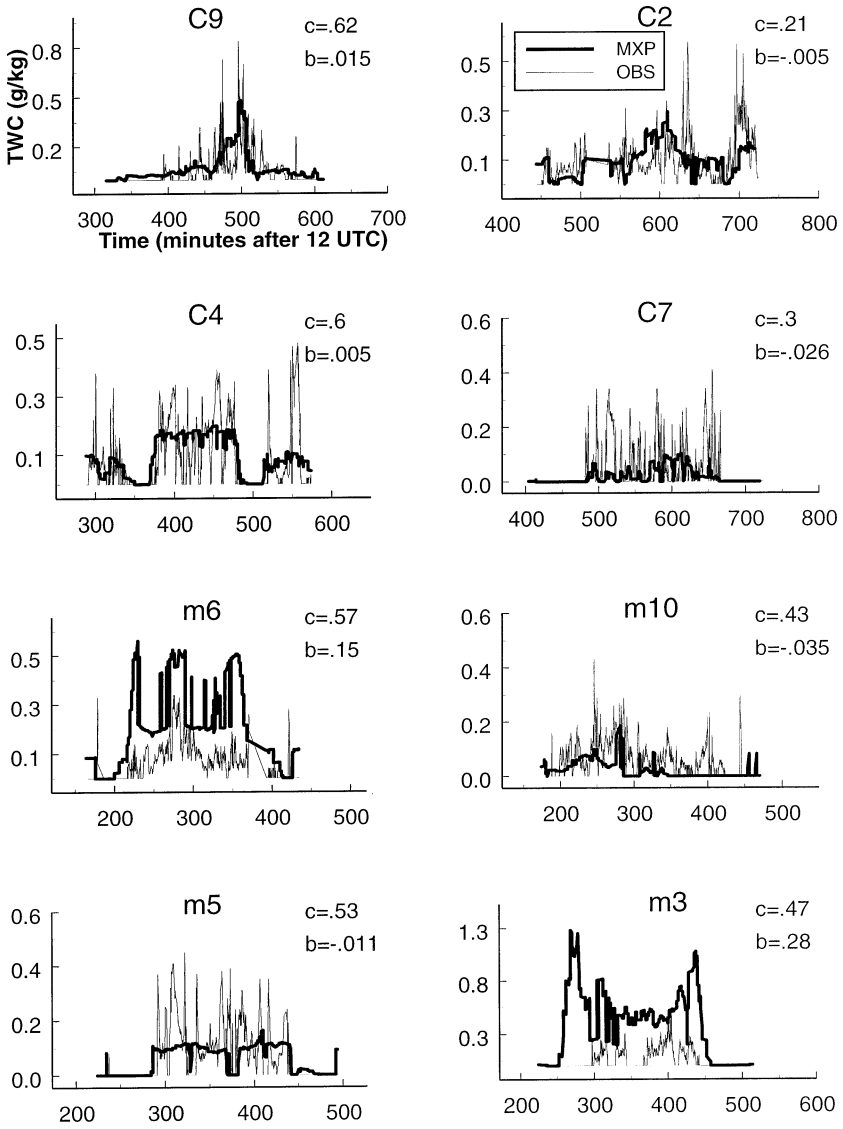

FIG. 5. Comparison of the observed (thin line) and modeled (thick line) time series of TWC for eight cases. The abscissa in all panels denotes time in minutes after 1200 UTC while the ordinate is TWC in units of g kg^{-1}. The correlation and bias (mean of model − mean of observations) is shown in the top-left corner of each panel.

Based on a detailed analysis of each case (using graphs such as Figs. 3 and 4) and on the descriptive statistics presented in Tables 1–3, it was found that for approximately half the flights, the observation–model comparison is encouraging. However, in several instances, there is clearly a timing difference between the observed and modeled meteorological situation that can explain a failed comparison. For example, there are no clouds along the virtual trajectory for case c8 although SLW and mixed-phase clouds were observed (Table 1). An examination of the *Geostationary Operational Environmental Satellite-8* (*GOES-8*) IR image (24 January 1998 at 1200 UTC) at approximately the time of the flight (1300–1700 UTC) shows that the aircraft sampled the northwest edge of a large mass of clouds associated with a synoptic storm. This storm is present in the model simulation but is situated slightly farther east.

A more comprehensive analysis of the results was obtained by comparing the real and virtual ''climatologies'' of the cloud types as well as of the water content: total, ice and supercooled. Clearly, no conclusion can be drawn on the quality of the microphysical scheme from cases where no clouds are present (along the virtual aircraft trajectory, for example). In order to avoid the conclusions being unduly influenced by such cases where the observation–model comparison is unsatisfactory, the five best maritime and the five best continental cases were selected in the following manner. For each

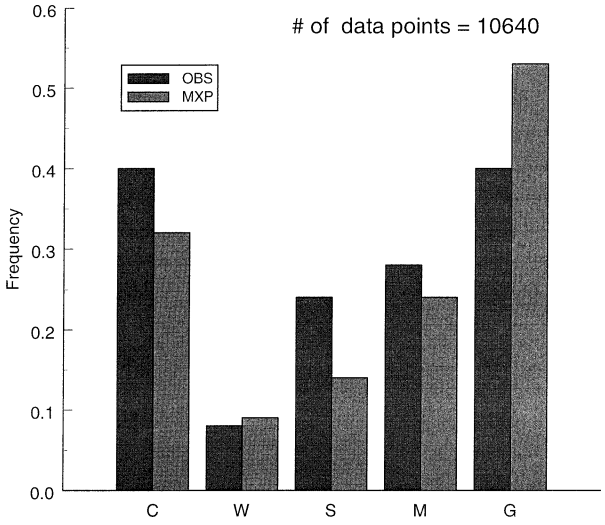

FIG. 6. The frequency of each cloudy type observed and modeled for the 10 selected cases. The letters C, W, S, M, and G stand for clear (TWC < 0.02 g kg^{-1}), warm (temperature $> 0°$), supercooled (no ice is present), mixed, and glaciated (no liquid is present), respectively. The frequency for clear data points is normalized with the total number of data points indicated in the top-right corner (same for observed and modeled data points), and the frequencies of the various cloudy types are normalized by the total number of nonclear data points (different for observed and modeled data points).

of the six variables shown in Tables 2 and 3, all maritime and all continental cases were sorted according to increasing correlation. For every variable, each case was assigned a score equal to its rank in this sorted list. Next, for each case, the scores of each variable were multiplied to obtain a number between 1 and 10^6 (10 continental cases and 6 variables) or 11^6 (11 maritime cases). In other words, a maritime case that would have the highest correlation for each of the six variables would end up with a score of 11^6. All maritime and continental cases are then ranked according to this single number and the five highest maritime and the five highest continental cases were selected for further analysis. These cases are c2, c3, c4, c7, c9, m1, m3, m5, m6, and m10. An examination of Tables 1–3 shows that for these 10 cases the model–observation comparisons were acceptable for all variables. The qualifier acceptable here is used to mean that there are no obvious quantitative reasons to disqualify any of these cases. Examining Table 1, we immediately see that cases c5, c8, m4, and m9 can be qualified as unacceptable because of the almost complete absence of predicted clouds along the flight trajectories. Other unacceptable cases can also be found by examining Tables 2 and 3 (e.g., negative correlations of TWC for cases m9, c1, c5, c8, and c10).

An illustration of the link between the correlations and the quality of the model–observation comparison can be found in Fig. 5. This shows a comparison of the observed and modeled time series of the TWC for eight of the selected cases. The panels are organized such that starting at the top-left corner and moving counterclockwise the correlation decreases. The correlation and the bias are indicated in the top right of each panel. It can be seen that for these cases the forecast of the presence of clouds was a success. However a strong bias in the actual TWC can be seen for certain cases, such as m3 and m6.

Figure 6 shows a histogram (similar to those of Fig. 1) of the frequency of each cloudy type observed as well as modeled for the 10 selected cases. The frequencies for clear data points are normalized with the total number of data points (same for observed and modeled data points), whereas the frequencies of the various cloudy types are normalized by the total number of nonclear data points (different for observed and modeled data points). Two features are apparent in this figure. First, there is an overestimation of the frequency of glaciated clouds. Second the presence of supercooled water is underestimated, particularly in ''pure'' supercooled liquid water clouds but also in mixed-phase clouds. The systematic nature of these two problems is also apparent in Table 1. This table shows, for every maritime and continental case, the number of observed and modeled data points of each cloudy type. An examination of this table for all cases, and for the selected cases, shows that these problems are not the result of a few severe cases but occur in the majority of cases. It should be noted that MXP has more ability in forecasting mixed-phase clouds than pure SLW events (liquid phase). The only way to have a pure SLW forecast in the MXP scheme is when the classical melting-ice mechanism is active. In MXP, the empirical algorithm of Huffman and Norman (1988) has been implemented to account for this mechanism. This algorithm diagnoses the phase of condensate based on empirical relationships involving the temperature profile (depth of warm and cold layers).

Figure 7 shows a comparison of the observed (OBS) and modeled (MXP) cumulative frequency of TWC, IWC, and supercooled liquid water content (SLWC) for the selected cases. For example, the top panel shows that 10% of observed data points of TWC have a water content between 0.02 and 0.04 g kg^{-1}. It can be seen that the model overestimates the frequency of high TWC (top panel), which can be attributed to an overestimation in the IWC (middle panel). A close examination of the IWC signal for all these cases revealed that this is mostly the result of significant overestimations of IWC in a few specific cases (e.g., see m3 and m6 in Table 3). However, an examination of Tables 3 and 4 clearly indicates that the MXP overestimates the IWC in a majority of cases. As discussed in Tremblay et al. (2001, 2003), this suggests that improvements are needed in the treatment of ice-particle microphysics in the MXP scheme. While the frequency distributions for the observed water contents fall monotonically (gradient of cumulative frequency decreases smoothly) as a function of increasing quantity, the modeled frequency distributions, in par-

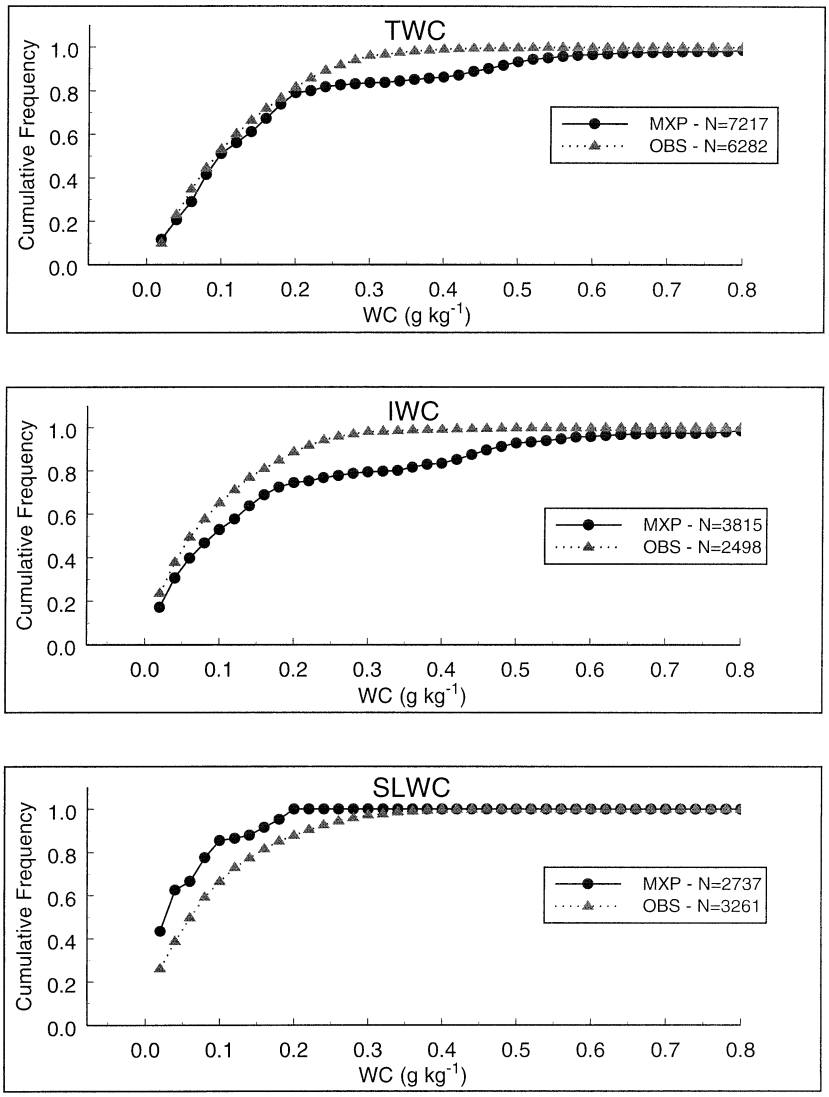

FIG. 7. Cumulative frequency distribution of the observed (OBS) and modeled (MXP) TWC, IWC, and SLWC for the 10 selected cases. The abscissa in all panels denotes the given water content in units of g kg^{-1} (accumulated by bin widths of 0.02 g kg^{-1}) while the ordinate denotes cumulative frequency, and *N* stands for the number of data points with nonzero water content of the given type.

ticular for the SLWC, are more structured. It can be seen that the model overestimates the frequency of very small quantities of SLWC with over 40% of its values in the lowest bin (0.02–0.04 g kg^{-1}). The model also underestimates the frequency of higher values of SLWC with frequencies of $\sim$0 for values $>$0.2 g kg^{-1}. This indicates that the parameterization of microphysics of liquid particles in the cloud model should be examined or adjusted in order to better represent natural clouds.

Figure 8 shows the LWC as a function of IWC for all data points identified as mixed phase. This plot combines two plots. One for the observed data points (circles), using the bottom and left axes, and one for the model data points (squares), using the top and right axes. As in Fig. 7, it can be seen that the MXP scheme has difficulties producing larger values of SLWC. These higher values can be crucial for aircraft icing forecasts. A clear cutoff of 0.1 g kg^{-1} in the modeled LWC of mixed-phase data points is also evident in Fig. 8. This problem is inherent in the Kessler-type parameterization that transforms cloud water in rainwater when the cloud water content reaches a certain threshold. Such a parameterization is used in the MXP scheme and a threshold of 0.1 g kg^{-1} was used in this study. It should be noted that increasing the value of this threshold results in more SLW in clouds. Work is under way to evaluate the sensitivity of the model climatology of LWC as well as the surface precipitation to this threshold.

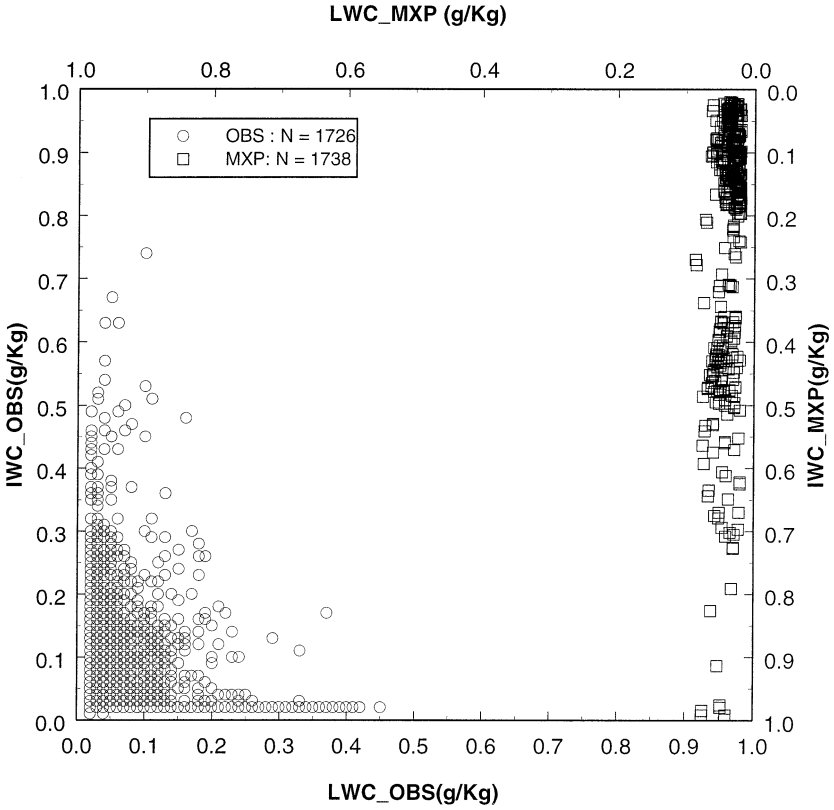

FIG. 8. LWC as a function of IWC for all data points identified as mixed phase among the 10 selected cases. The observed data points (denoted with circles) are plotted with respect to the bottom and left axes while the model data points (denoted with squares) are plotted with respect to the top and right axes.

Figure 9 shows the frequency distribution of the fractional ice water content (IWC/TWC) for all observed and modeled mixed-phase data points of the 10 selected cases. It can be seen that for most modeled data points the ice phase is strongly dominant, while for the observed data points the frequency distribution is flatter with a minimum at a fractional ice water content of 0.5. Cober et al. (2001a) and Korolev et al. (2002) showed similar observations. Thus, MXP failed to reproduce the *climatology* of the ice and liquid phase partition within mixed-phase clouds, emphasizing again that an optimization of the scheme based on observations within clouds is mandatory producing better predictions of cloud microphysics properties.

6. Conclusions

In order to provide guidance for the further improvement of the mixed-phase cloud scheme of Tremblay et al. (1996), comparisons of dynamical, thermodynamical, as well as microphysical variables between in situ aircraft data and model data were made. A total of 21 flights (~88 h of data) from the First and Third Canadian Freezing Drizzle Experiments were selected and simulated. The basis of the evaluation of the model performance is a point-by-point comparison of each pertinent variable along the real and ''virtual'' aircraft trajectories. The virtual aircraft trajectory is constructed by choosing, for every observed data point, the closest available model data point in terms of time, pressure level, and latitude–longitude position. Observed and model data were used to calculate detailed descriptive statistics to evaluate the ability of the forecast system in predicting cloud microphysics.

In this model–observation comparison as in most similar work, two issues (discussed at length in previous sections) must be kept in mind that constrain the generality of the conclusions. One is the disparity in temporal and spatial resolution between the observations and the model. The other is the difficulty of distinguishing between the effects of the dynamics and those that can be imputed to a specific physical parameterization (namely the microphysics).

We now answer the questions formulated in section 2.

1) The quality of the model simulations in terms of the presence of clouds were found to be encouraging for about half the flights simulated. It was found that it is more challenging to predict the water content variables than the dynamic variables. It was found that

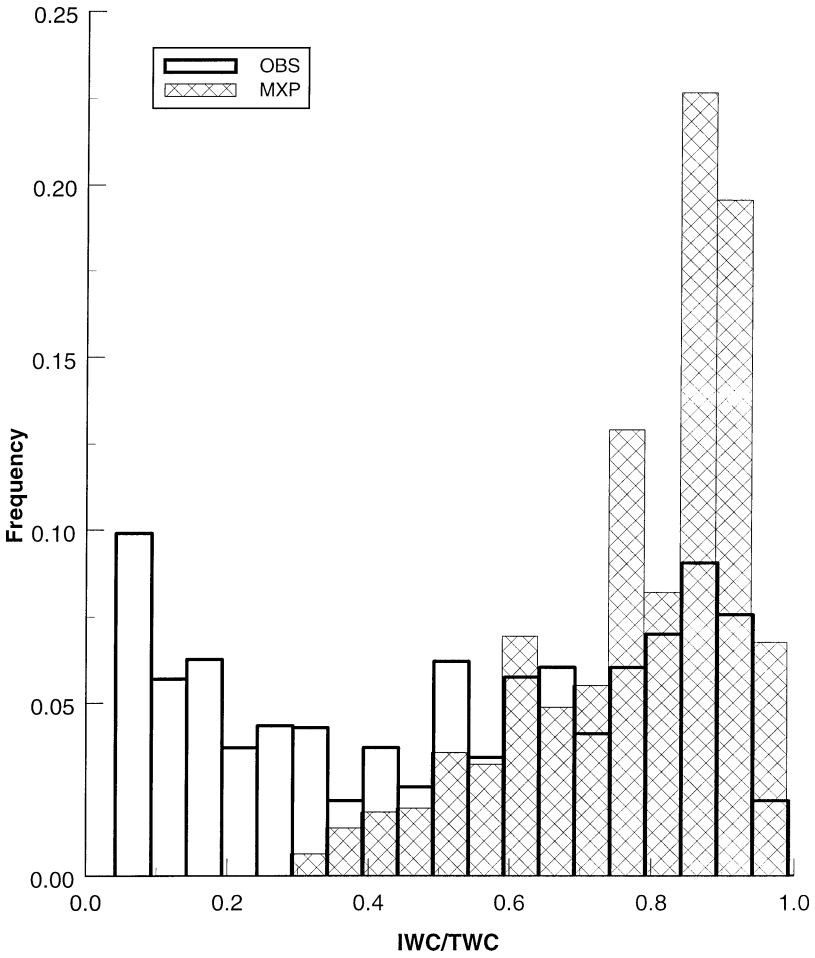

FIG. 9. Frequency distribution of the fractional ice water content (IWC/TWC) for all OBS and MXP mixed-phase data points of the 10 selected cases. Bin width is 0.05.

the MXP scheme overpredicts (underpredicts) the frequency of glaciated (supercooled) clouds.

2) It was found that the model predicts ice clouds better than water clouds. The model generally overpredicts (underpredicts) the quantities of IWC (SLW).
3) Where mixed phase is present in the model, the ice phase represents a large fraction of the TWC, contrary to the observations.

These findings suggest three weaknesses of the MXP cloud scheme that can be improved: 1) underforecast of the presence of mixed phase clouds as well as of the intensity of SLW in these clouds, 2) general underforecast of the presence of pure SLW clouds as well as of the intensity of SLW in these clouds, and 3) general overforecast of glaciated clouds and overforecast of ice water content in mixed-phase clouds.

Underscoring the generality of these conclusions, Guan et al. (2002) came to similar conclusions using a different dynamical model and a different aircraft–model comparison strategy. These weaknesses can be directly linked to the lack of understanding of several microphysical processes such as primary and secondary activation of ice, the collision–coalescence process, as well as to the inherent difficulties in parameterizing these highly subgrid-scale processes. For example, points 1 and 3 are likely related to specific aspects of the microphysics of ice particles and their interaction with supercooled liquid water droplets. Point 2 suggests that adjustments to the ice activation parameterization might be necessary. Based on the conclusions stated above, Tremblay et al. (2003) propose some modifications to the parameterization of the ice particle size distribution used in the MXP cloud scheme that resulted in improvements of the forecast of SLW relative to IWC.

Acknowledgments. The authors would like to acknowledge the financial support of the National Search and Rescue Secretariat, Transport Canada, and the Boeing commercial airplane group. The technical and scientific staff of MSC and the National Research Council of Canada (NRC) are acknowledged for their support in making measurements with the NRC Convair-580 research aircraft.

REFERENCES

Ashenden, R., and J. D. Marwitz, 1998: Characterizing the supercooled large droplet environment with corresponding turboprop aircraft response. *J. Aircraft,* **35,** 912–920.

Benoit, R., M. Desgagne, P. Pellerin, S. Pellerin, Y. Chartier, and S. Desjardins, 1997: The Canadian MC2: A semi-Lagrangian, semi-implicit wideband atmospheric model suited for finescale process studies and simulation. *Mon. Wea. Rev.,* **125,** 2382–2415.

Bourgouin, P., 2000: A method to determine precipitation type. *Wea. Forecasting,* **15,** 583–592.

Brown, B. G., G. Thompson, R. T. Bruintjes, R. Bullock, and T. Kane, 1997: Intercomparison of in-flight icing algorithms. Part II: Statistical verification results. *Wea. Forecasting,* **12,** 890–914.

Cober, S. G., J. W. Strapp, and G. A. Isaac, 1996: An example of supercooled drizzle drops formed through a collision–coalescence process. *J. Appl. Meteor.,* **35,** 2250–2260.

——, G. A. Isaac, A. V. Korolev, and J. W. Strapp, 2001a: Assessing cloud-phase conditions. *J. Appl. Meteor.,* **40,** 1967–1983.

——, ——, and J. W. Strapp, 2001b: Characterizations of aircraft icing environments that include supercooled large droplets. *J. Appl. Meteor.,* **40,** 1984–2002.

Cortinas, J., Jr., 2000: A climatology of freezing rain in the Great Lakes region of North America. *Mon. Wea. Rev.,* **128,** 3574–3588.

Guan, H., S. G. Cober, and G. A. Isaac, 2001: Verification of supercooled cloud water forecasts with in situ aircraft measurements. *Wea. Forecasting,* **16,** 145–155.

——, ——, ——, A. Tremblay, and A. Méthot, 2002: Comparions of three cloud forecast schemes with in situ aircraft measurements. *Wea. Forecasting,* **17,** 1226–1235.

Heymsfield, J. A., and L. M. Miloshevich, 1993: Homogeneous ice nucleation and supercooled liquid water in orographic wave clouds. *J. Atmos. Sci.,* **50,** 2335–2355.

Hobbs, P. V., and A. L. Rangno, 1985: Ice particle concentrations in clouds. *J. Atmos. Sci.,* **23,** 2523–2549.

Huffman, G. J., and G. A. Norman, 1988: The supercooled warm rain process and the specification of freezing precipitation. *Mon. Wea. Rev.,* **116,** 2172–2182.

Isaac, G. A., S. G. Cober, A. V. Korolev, J. W. Strapp, and A. Tremblay, 1998: Overview of the Canadian Freezing Drizzle Experiment I, II and III. Preprints, *Conf. on Cloud Physics,* Everett, WA, Amer. Meteor. Soc., 447–450.

——, ——, J. W. Strapp, A. V. Korolev, A. Tremblay, and D. L. Marcotte, 2001: Recent Canadian research on aircraft in-flight icing. *Can. Aeronaut. Space J.,* **47** (3), 213–221.

Khain, A., M. Ovtchinnikov, M. Pinsky, A. Pokrovsky, and H. Krugliak, 2000: Notes on the state of the art numerical modeling of cloud microphysics. *Atmos. Res.,* **55,** 159–224.

Korolev, A. V., G. A. Isaac, S. G. Cober, and J. W. Strapp, 2002: Observation of the microstructure of mixed phase clouds. *Quart. J. Roy. Meteor. Soc.,* in press.

Laroche, S., P. Gauthier, J. St-James, and J. Momeau, 1999: Implementation of a 3D variational data assimilation system at the Canadian Meteorological Center. Part II: The regional analysis. *Atmos.–Ocean,* **37,** 103–156.

Marwitz, J., M. Politovich, B. Bemstein, F. Ralph, P. Neiman, R. Ashenden, and J. Bresch, 1997: Meteorological conditions associated with the ATR72 aircraft accident near Roselawn, Indiana, on 31 October 1994. *Bull. Amer. Meteor. Soc.,* **78,** 41–52.

Politovich, M. K., 1989: Aircraft icing caused by large supercooled droplets. *J. Appl. Meteor.,* **28,** 856–868.

Rauber, R. M., and L. O. Grant, 1986: The characteristics and distribution of cloud water over the mountains of northern Colorado during wintertime storms. Part II: Spatial distribution and microphysical characteristics. *J. Appl. Meteor.,* **25,** 489–504.

——, L. S. Olthoff, and M. K. Ramamurthy, 2000: The relative importance of warm rain and melting processes in freezing precipitation events. *J. Appl. Meteor.,* **39,** 1185–1195.

Reagan, M., 1998: Canadian ice storm 1998. *World Meteorological Organization Bulletin,* Vol. 47, No. 3, 250–256.

Rosenfeld, D., and I. M. Lensky, 1998: Satellite-based insights into precipitation formation processes in continental and maritime convective clouds. *Bull. Amer. Meteor. Soc.,* **79,** 2457–2476.

Sand, W. R., W. A. Cooper, M. K. Politovich, and D. L. Veal, 1984: Icing conditions encountered by a research aircraft. *J. Appl. Meteor.,* **23,** 1427–1440.

Sassen, K., K. N. Liou, S. Kinne, and M. Griffin, 1985: Highly supercooled cirrus cloud water: Confirmation and climatic implications. *Science,* **227,** 411–413.

Strapp, J. W., R. A. Stuart, and G. A. Isaac, 1996: A Canadian climatology of freezing precipitation and a detailed study using data from St John's, Newfoundland. *Proc. Int. Conf. on Inflight Aircraft Icing,* Vol. II, Springfield, VA, Federal Aviation Administration DOT/FAA/AR-96/81 II, 45–56.

Stuart, R. A., and G. A. Isaac, 1999: Freezing precipitation in Canada. *Atmos.–Ocean,* **37,** 87–102.

Tremblay, A., and A. Glazer, 2000: An improved modeling scheme for freezing precipitation. *Mon. Wea. Rev.,* **128,** 1289–1308.

——, ——, W. Szyrmer, G. A. Isaac, and I. Zawadzki, 1995: Forecasting of supercooled clouds. *Mon. Wea. Rev.,* **123,** 2098–2113.

——, ——, W. Yu, and R. Benoit, 1996: A mixed-phase cloud scheme based on a single prognostic equation. *Tellus,* **48A,** 483–500.

——, ——, and L. Garand, 2001: Comparison of three cloud schemes in winter storm forecasts. *Mon. Wea. Rev.,* **129,** 1923–1938.

——, P. A. Vaillancourt, S. G. Cober, A. Glazer, and G. A. Isaac, 2003: Improvements of a mixed-phase cloud scheme using aircraft observations. *Mon. Wea. Rev.,* **131,** 672–686.